hibiting this unusual coordination geometry.

Conclusion

The ground-state conformations of (cyclopentadienyl)-titanium(IV) and -titanium(III) complexes are predominantly influenced by electronic factors. The ground-state structures in the titanium(IV) series are characterized by a lesser positive charge on the titanium, and where enough electrons exist through ligand–metal bonding, these structures are 16e species. This study has provided valuable insight into alternative coordination modes of the Cp ligand. A detailed study of the η^2-coordination geometry allows us to predict a means of stabilizing this unusual bonding mode. Substitution of hydrogen with π-donating groups such as F, OH, or OCH_3 at positions C_3 and C_4 of the Cp ligand could enhance the η^2-bonding capability by stabilizing the allyl cation-like character of carbons three through five. A challenge can now be made to the experimentalist to synthesize new η^2-coordinating compounds.

Acknowledgment. We thank the Robert A. Welch Foundation (Grant Y-743) and the Organized Research Fund of the University of Texas at Arlington for their support of this work. Computer time was provided by the University of Texas System Center for High Performance Computing.

Registry No. Cl_3CpTi, 1270-98-0; Cl_2Cp_2Ti, 1271-19-8; $ClCp_3Ti$, 11079-20-2; Cp_4Ti, 11079-32-6; Cp_3Ti, 52700-41-1.

Activation of 1-Alkynes at 16-Electron Rhodium Fragments. Some Examples of Thermodynamically Favored Rearrangements [M(π-HC≡CR)] → [M(H)(C≡CR)]

Claudio Bianchini,*,† Dante Masi,† Andrea Meli,† Maurizio Peruzzini,† José A. Ramirez,‡ Alberto Vacca,† and Fabrizio Zanobini†

Istituto per lo Studio della Stereochimica ed Energetica dei Composti di Coordinazione, ISSECC CNR, Via J. Nardi 39, 50132 Firenze, Italy, and Department of Chemistry, University of Valencia, Valencia, Spain

Received February 3, 1989

The 16-electron fragments $[(NP_3)Rh]^+$ and $[(PP_3)Rh]^+$ react with 1-alkynes in THF at room temperature yielding Rh(III) cis hydride acetylide complexes of formula $[(L)Rh(H)(C{\equiv}CR)]BPh_4$ [L = NP_3, $N(CH_2CH_2PPh_2)_3$; L = PP_3, $P(CH_2CH_2PPh_2)_3$; R = H, n-C_3H_7, Ph, $SiMe_3$, CH_2OH, CHO, CO_2H, CO_2Et]. The crystal structure of the ethynyl derivative $[(NP_3)Rh(H)(C{\equiv}CH)]BPh_4{\cdot}1.5THF$ was determined by X-ray crystallography. The metal atom in the complex cation is octahedrally coordinated by the four donor atoms of NP_3, a σ-bonded ethynyl group, and a hydride ligand. Crystal data: monoclinic, space group $P2_1/n$, a = 15.769 (3) Å, b = 32.458 (6) Å, c = 13.277 (6) Å; β = 105.21 (2)°, U = 6557 (1) Å^3; Z = 4. The structure was solved by Patterson and Fourier techniques and refined to an R factor of 0.079 (R_w = 0.086) by using 3735 reflections with $I > 3\sigma(I)$. Decreasing the temperature to −40 °C does not change the nature of the products except for the reactions with $HC{\equiv}CCO_2Et$. In this case, the π-alkyne adducts $[(L)Rh(\pi\text{-}HC{\equiv}CCO_2Et)]BPh_4$ (L = NP_3, PP_3) are formed which are thermodynamically unstable in ambient temperature solutions to irreversibly give the corresponding hydride acetylide derivatives. The $[Rh(\pi\text{-}HC{\equiv}CCO_2Et)] \rightarrow [Rh(H)(C{\equiv}CCO_2Et)]$ rearrangement is preceded at lower temperature by a fluxional process on the ^{31}P NMR time scale which involves the π-alkyne species. At low temperature, also propiolic acid, $HC{\equiv}CCO_2H$, forms with the $[(NP_3)Rh]^+$ fragment a π-alkyne complex which converts, in ambient temperature solutions, into hydride acetylide and hydride carboxylate derivatives via two independent, almost equally favored pathways. Most of the hydride acetylide complexes of rhodium(III) react with excess $NaBH_4$ in THF/ethanol yielding Rh(I) σ-acetylides of formula $[(L)Rh(C{\equiv}CR)]$ (R = n-C_3H_7, Ph, $SiMe_3$, CH_2OH, CO_2Et, CHO). No interconversion between the NP_3 hydride acetylide complexes and the parent vinylidenes $[(NP_3)Rh\{C{=}C(H)(R)\}]BPh_4$ was observed.

Introduction

The stoichiometric reactions between terminal alkynes and unsaturated metal fragments give different products depending on the alkyne and metal components. In cases of ethyne or of alkynes bearing inert substituents like aryl or alkyl groups, three species can be isolated: π-alkyne, hydride acetylide, or vinylidene complexes.[1] While it is generally agreed that the initial interaction between the metal system and the alkyne molecule is of the π-type and that only at a later stage, the π-intermediate eventually converts into hydride acetylide or vinylidene derivatives,[1c-i] there are still doubts about the whys and mechanism of the metal–π-alkyne degradation. In particular, it is not completely established whether the hydride acetylide system is a precursor to the vinylidene functionality as it

†ISSECC, CNR.
‡University of Valencia.

(1) (a) Nelson, J. H.; Jonassen, H. B.; Roundhill, D. M. *Inorg. Chem.* **1969**, *8*, 2591. (b) Bennett, M. A.; Charles, R.; Fraser, P. J. *Aust. J. Chem.* **1977**, *30*, 1213. (c) Werner, H.; Höhn, A. *J. Organomet. Chem.* **1984**, *272*, 105. (d) Garcia Alonso, F. J.; Hohn, A.; Wolf, J.; Otto, H.; Werner, H. *Angew. Chem., Int. Ed. Engl.* **1985**, *24*, 406. (e) Wolf, J.; Werner, H.; Serhadli, O.; Ziegler, M. L. *Ibid.* **1983**, *22*, 414. (f) Werner, H.; Wolf, J.; Garcia Alonso, F. J.; Ziegler, M. L.; Serhadli, O. *J. Organomet. Chem.* **1987**, *336*, 397. (g) Werner, H.; Garcia Alonso, F. J.; Otto, H.; Wolf, J. *Z. Naturforsch., B* **1988**, *43B*, 722. (h) Birk, R.; Grossmann, U.; Hund, H.-U.; Berke, H. *J. Organomet. Chem.* **1988**, *345*, 321. (i) Birk, R.; Berke, H.; Huttner, G.; Zsolnai, L. *Chem. Ber.* **1988**, *121*, 471. (j) Bullock, R. M. *J. Chem. Soc., Chem. Commun.* **1989**, 165.

0276-7333/89/2308-2179$01.50/0

Scheme I

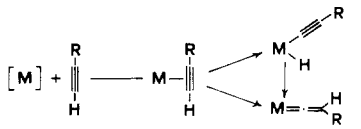

has been claimed for a few cases[1d-g,4] or whether the alkyne–vinylidene rearrangement directly occurs via a formal 1,2-hydrogen shift as it has been proposed on theoretical grounds by Silvestre and Hoffmann (Scheme I).[2]

When the terminal alkynes bear substituents with potentially activable element–hydrogen bonds like the C–H and O–H bonds of the –CHO, –COOH, and $-CH_2OH$ groups, the alternative reaction of the metal fragment with the substituent may compete or even prevail over sp C–H bond cleavage.[3] As the alternative reaction with the substituent is responsible for several catalytic transformations of 1-alkynes,[3] it appears extremely important to know as much as possible on the factors that may control the activation of C–H vs other element–H bonds.

In an attempt to gain further insight into the metal chemistry of terminal alkynes, we have studied the reactions of a variety of 1-alkynes with the coordinatively and electronically unsaturated metal fragments $[(NP_3)Rh]^+$ and $[(PP_3)Rh]^+$ [NP_3 = $N(CH_2CH_2PPh_2)_3$; PP_3 = $P(CH_2CH_2PPh_2)_3$]. Since we have been able to isolate most of the species that are potentially obtainable by stoichiometrically reacting a terminal alkyne with a metal system i.e. η^2-alkyne, hydride acetylide, and σ-acetylide derivatives or compounds derived from the alternative activation of the alkyne substituent, we have now a good chance to correlate the nature of the products obtained with the alkyne and metal components and the reaction conditions as well.

A preliminary account of part of this work has already appeared.[4]

Experimental Section

General Data. Tetrahydrofuran (THF) was purified by distillation over $LiAlH_4$ under nitrogen just prior to use. All the other solvents were reagent grade and were used as received. The compounds $[(NP_3)RhH]$ (1) and $[(PP_3)RhH]$ (2) were prepared as described in ref 5. Alkynes were purchased from commercial suppliers and used without further purification. Propargylaldehyde was prepared according to the method reported by Sauer.[6] The ligand NP_3 was synthesized as previously described.[7] The ligand PP_3 was purchased from Pressure Chemicals. Infrared spectra were recorded on a Perkin-Elmer 283 spectrophotometer using samples mulled in Nujol between KBr plates. Proton NMR spectra were recorded at 299.945 MHz on a Varian VXR 300 spectrometer. Peak positions are relative to tetramethylsilane as external reference. $^{31}P\{^1H\}$ NMR spectra were recorded on Varian CFT 20 and Varian VXR 300 instruments operating at 32.19 and 121.42 MHz, respectively. Chemical shifts are relative to external H_3PO_4 85% with downfield values reported as positive. Conductivities were measured with a WTW Model LBR/B conductivity bridge. The conductivity data were obtained at sample concentrations of ca. 1×10^{-3} M in nitroethane solutions. GC analyses were performed on a Shimadzu GC-8A gas chromatograph fitted with a thermal conductivity detector and a 10-ft 100/120 Carbosieve-SII stainless-steel column (Supelco Inc.). Quantification was achieved with a Shimadzu C-R6A Chromatopac coupled with the chromatograph, operating with an automatic correct area normalization method.

Simulation of NMR spectra was achieved by using an updated version of the LAOCN4 program.[8] The initial choices of shifts and coupling constants were refined by successive iterations, the assignment of the experimental lines being performed automatically. The final parameters gave a fit to the observed line positions better than 0.6 Hz.

Synthesis of the Complexes. All reactions and manipulations were routinely performed under a prepurified nitrogen or argon atmosphere by using Schlenk line techniques. The solid compounds were collected on sintered glass frits and washed, unless otherwise stated, with ethanol and *n*-pentane before being dried in a stream of nitrogen.

Conductivity values and selected IR absorbances for all of the compounds are reported in Table I. Yields and microanalytical data are reported in Table II. Selected NMR data for all of the new complexes are collected in Table III (^1H NMR spectra) and Table IV ($^{31}P\{^1H\}$ NMR spectra).

Preparation of $[(NP_3)Rh(H)(C{\equiv}CH)]BPh_4$ (3). To a stirred suspension of 1 (0.30 g, 0.40 mmol) in THF (25 mL) was added via syringe $MeOSO_2CF_3$ (60 μL, 0.54 mmol) at 0 °C. In a few minutes the yellow hydride dissolved to produce a colorless solution, in which ethyne was bubbled until the solution became

Table I. Infrared and Conductivity Data for the Complexes

complex	Λ,[a] Ω^{-1} cm^2 mol^{-1}	IR, cm^{-1} ν(RhH)	ν(C≡C)	other
3	54	2015	1975	ν(CH) 3275
4	52	1970	2010	
5	52	2000	2120	
6	55	2025	2045	ν(SiC) 855
7	54	2010	2110	ν(OH) 3330
8	50	2050	2100	ν(CO) 1630
9	53	2050	2110	ν(CO) 1690 ν(COEt) 1210
10	54	1990	2090	ν(CO) 1670
11	56	2020	2120	ν(CO) 1625
12	52	2050	1970	ν(CH) 3280
13	50	1990	2015	
14	56	2045	2115	
15	55	2000	2040	ν(SiC) 845
16	53	2005	2100	
17	54	2000	2085	ν(CO) 1630
18	53	2030	2065	ν(CO) 1680 1640
19	53	2015	2105	ν(CO) 1680 ν(COEt) 1210
20	64[b]		1780	ν(CO) 1690 ν(COEt) 1210
21	58[b]		1785	ν(CO) 1670 ν(COEt) 1210
22	c		2100	
23	c		2080	
24	c		2010	ν(SiC) 870
25	c		2095	
26	c		2050	ν(CO) 1660 ν(COEt) 1195
27	c		2100	
28	c		2070	
29	c		2010	ν(SiC) 860
30	c		2080	
31	c		2070	ν(CO) 1595
32	c		2050	ν(CO) 1655 ν(COEt) 1180

[a] In ca. 1×10^{-3} M nitroethane solutions unless otherwise stated. [b] In ca. 1×10^{-3} M dichloromethane solution. [c] Nonelectrolyte in nitroethane or dichloromethane solutions.

(2) Silvestre, J.; Hoffmann, R. *Helv. Chim. Acta* **1985**, *68*, 1461.
(3) (a) Marder, T. B.; Chan, D. M.-T.; Fultz, W. C.; Calabrese, J. C.; Milstein, D. *J. Chem. Soc., Chem. Commun.* **1987**, 1885. (b) Marder, T. B.; Chan, D. M.-T.; Fultz, C. F.; Milstein, D. *Ibid.* **1988**, 996. (c) Marder, T. B.; Zargarian, D.; Calabrese, J. C.; Herskowitz, T. H.; Milstein, D. *Ibid.* **1987**, 1484.
(4) Bianchini, C.; Mealli, C.; Peruzzini, M.; Vizza, F.; Zanobini *J. Organomet. Chem.* **1988**, *346*, C53.
(5) Bianchini, C.; Masi, D.; Meli, A.; Peruzzini, M.; Zanobini, F. *J. Am. Chem. Soc.* **1988**, *110*, 6411.
(6) Sauer, J. C. *Organic Syntheses*; Wiley: New York, 1962; Coll. Vol. 4, p 812.
(7) Morassi, R.; Sacconi, L. *Inorg. Synth.* **1976**, *16*, 174.
(8) Castellano, S.; Bothner-By, A. A. *J. Chem. Phys.* **1964**, *41*, 3863.

Table II. Analytical Data for the Complexes

complex	yield, %	anal. found[a] C	H	N	Rh
3	80	73.72 (74.12)	5.98 (5.85)	1.10 (1.27)	9.16 (9.34)
4	85	74.29 (74.55)	6.21 (6.17)	1.16 (1.22)	8.79 (8.99)
5	80	75.15 (75.45)	5.85 (5.82)	1.20 (1.19)	8.49 (8.73)
6	85	72.61 (72.63)	6.26 (6.18)	1.02 (1.19)	8.63 (8.76)
7	70	73.07 (73.21)	6.01 (5.88)	1.17 (1.24)	8.99 (9.09)
8	60	73.46 (73.35)	5.80 (5.71)	1.03 (1.24)	8.94 (9.11)
9	80	72.48 (72.64)	5.95 (5.84)	1.06 (1.19)	8.49 (8.77)
10	42[b]	71.87 (72.32)	5.46 (5.63)	1.20 (1.22)	8.39 (8.98)
11	28[b]	72.04 (72.32)	5.70 (5.63)	1.09 (1.22)	8.43 (8.98)
12	85	72.97 (73.00)	5.81 (5.77)		9.12 (9.20)
13	70	73.29 (73.46)	6.03 (6.08)		8.80 (8.86)
14	85	74.39 (74.38)	5.70 (5.74)		8.49 (8.61)
15	75	71.42 (71.60)	6.17 (6.09)		8.55 (8.64)
16	75	72.06 (72.14)	5.60 (5.79)		8.87 (8.96)
17	55	71.95 (72.14)	5.84 (5.79)		8.72 (8.96)
18	60	71.07 (71.27)	5.52 (5.55)		8.80 (8.85)
19	90	71.63 (71.61)	5.49 (5.42)		8.51 (8.64)
20	90	56.86 (57.43)	4.99 (4.82)	1.21 (1.40)	10.06 (10.25)
21	90	55.99 (56.48)	4.72 (4.74)		10.02 (10.08)
22	45	68.09 (68.53)	5.88 (6.00)	1.60 (1.70)	12.32 (12.49)
23	50	69.86 (70.01)	5.56 (5.52)	1.61 (1.63)	11.97 (12.00)
24	60	65.94 (66.11)	5.89 (6.02)	1.49 (1.64)	11.92 (12.05)
25	55	66.46 (66.59)	5.67 (5.59)	1.63 (1.73)	12.49 (12.68)
26	65	66.09 (66.12)	5.62 (5.55)	1.55 (1.64)	11.99 (12.05)
27	50	67.02 (67.15)	5.93 (5.87)		12.09 (12.24)
28	65	68.46 (68.65)	5.49 (5.42)		11.67 (11.76)
29	65	64.82 (64.83)	5.96 (5.90)		11.78 (11.82)
30	60	65.09 (65.23)	5.40 (5.47)		12.23 (12.42)
31	50	65.12 (65.38)	5.21 (5.24)		12.29 (12.45)
32	70	64.70 (64.84)	5.51 (5.44)		11.68 (11.82)

[a] Calculated values are given in parentheses. [b] Total yield based on 1, 70%. See Experimental Section.

pale yellow (ca. 20 min). Pale yellow crystals separated after addition of solid $NaBPh_4$ (0.40 g, 1.17 mmol) and ethanol (25 mL).

Preparation of [(NP_3)Rh(H)(C≡CR)]BPh_4 [R = C_3H_7 (4), Ph (5), $SiMe_3$ (6), CH_2OH (7), CHO (8), CO_2Et (9)]. A slight excess (0.44 mmol) of the appropriate terminal alkyne was added to a THF solution of $[(NP_3)Rh]^+$ (0.40 mmol) prepared as above. The resulting pale yellow solution was stirred for 1 h at room temperature. On addition of solid $NaBPh_4$ (0.40 g, 1.17 mmol) to the resulting solution, followed by slow evaporation of the solvent, colorless or pale yellow crystals of the hydrido acetylido complexes **4–9** were obtained.

Reaction of [(NP_3)RhH] with $MeOSO_2CF_3$ and HC≡CC-O_2H. Addition of a slight excess of neat propiolic acid (27.5 μL, 0.44 mmol) to a colorless THF solution of $[(NP_3)Rh]^+$ (0.40 mmol) prepared as above gave after usual workup a mixture of [(NP_3)Rh(H)(C≡CCO_2H)]BPh_4 (**10**) and [(NP_3)Rh(H)(O_2CC≡CH)]BPh_4 (**11**) in ca. 3:2 ratio. Total yield based on **1**: ca. 70%. Pure samples of the compounds were obtained by chromatography in air on silica gel thick-layer plates (eluent CH_2Cl_2–methanol).

Preparation of [(PP_3)Rh(H)(C≡CH)]BPh_4 (12). A deep red solution of $[(PP_3)Rh]^+$ was prepared by adding via syringe 65 μL (0.59 mmol) of $MeOSO_2CF_3$ to a solution of **2** (0.40 g, 0.52 mmol) in THF (25 mL). Ethyne was bubbled into this solution until the color changed from deep red to colorless. Crystals of **12** began to separate after addition of solid $NaBPh_4$ (0.40 g, 1.17 mmol) and ethanol (25 mL) by slow concentration of the solution.

Preparation of [(PP_3)Rh(H)(C≡CR)]BPh_4 [R = C_3H_7 (13), Ph (14), $SiMe_3$ (15), CH_2OH (16), CHO (17), CO_2H (18), CO_2Et (19)]. The appropriate 1-alkyne was added in a slight excess to the deep red solution of $[(PP_3)Rh]^+$ prepared as above, which, immediately, turned colorless. On addition of solid $NaBPh_4$ (0.40 g, 1.17 mmol) and ethanol (25 mL) to the resulting solutions, followed by slow concentration, pale yellow crystals of **13–19** separated.

Preparation of [(NP_3)Rh(HC≡CCO_2Et)](SO_3CF_3) (20). A stirred THF (25 mL) suspension of **1** (0.30 g, 0.40 mmol) was treated with 50 μL (0.45 mmol) of $MeOSO_2CF_3$ at 0 °C. Within a few minutes, the starting hydride dissolved to produce a colorless solution which was cooled to −40 °C with a calcium chloride brine (30.5% $CaCl_2$). To this solution was added ethyl propiolate (44 μL, 0.44 mmol) which caused a color change from colorless to pale orange. On addition of cold *n*-hexane (50 mL), pale orange microcrystals of **20** separated. They were collected by filtration and washed with cold *n*-pentane (2 × 25 mL) before being dried in a stream of nitrogen.

Preparation of [(PP_3)Rh(HC≡CCO_2Et)](SO_3CF_3) (21). Compound **21** was prepared by the same procedure used to synthesize **20** but replacing **1** with **2**.

Reactions of [(NP_3)Rh(H)(C≡CR)]BPh_4 with $NaBH_4$ (R = C_3H_7, Ph, $SiMe_3$, CH_2OH, CO_2Et). A large excess of $NaBH_4$ (0.40 g, 10.51 mmol) dissolved in ethanol (20 mL) was added portionwise to a boiling THF solution (40 mL) of the appropriate cis hydride acetylide complex (ca. 0.2 mmol). The reflux was maintained for 12 h, and then the yellow solution was cooled to room temperature. Yellow crystals of the σ-acetylides [(NP_3)-Rh(C≡CR)] [R = *n*-C_3H_7 (**22**), Ph (**23**), $SiMe_3$ (**24**), CH_2OH (**25**), CO_2Et (**26**)] precipitated by addition of ethanol. The yields ranged from 45% to 65%.

Reaction of [(NP_3)Rh(H)(C≡CH)]BPh_4 with $NaBH_4$. When the hydride acetylide derivative **3** (0.20 g, 0.18 mmol) was reacted with excess of ethanolic $NaBH_4$ as described above, yellow crystals of **1**, instead of the expected σ-ethynyl complex [(NP_3)Rh(C≡CH)], were obtained in ca. 60% yield.

Reactions of [(PP_3)Rh(H)(C≡CR)]BPh_4 with $NaBH_4$ (R = C_3H_7, Ph, $SiMe_3$, CH_2OH, CHO, CO_2Et). The σ-acetylides derivatives [(PP_3)Rh(C≡CR)] [R = C_3H_7 (**27**), Ph (**28**), $SiMe_3$ (**29**), CH_2OH (**30**), CHO (**31**), CO_2Et (**32**)] were prepared in a fashion similar to that above described for the NP_3 analogues by reacting the corresponding cis hydrido acetylide complexes with excess $NaBH_4$ in ethanol. The yields ranged from 50% to 70%.

Reaction of [(PP_3)Rh(H)(C≡CH)]BPh_4 with $NaBH_4$. The hydride **2** was obtained in 65% yield by substituting **12** for **3**.

Reactions of [(L)Rh(H)(C≡CR)]BPh_4 (L = NP_3, R = CHO, CO_2H; L = PP_3, R = CO_2H) with $NaBH_4$. Reaction of the hydride acetylide complexes **8**, **10**, and **18** with $NaBH_4$ as described above did not give reproducible results. Extensive decomposition of the complex species occurred, and the only isolable products were intractable powders.

X-ray Data Collection and Structure Determination of 3·1.5THF. Crystals suitable for an X-ray diffraction analysis were obtained by slow diffusion of ethanol vapors into a THF solution of **3** maintained under a nitrogen atmosphere at room temperature.

Table III. Selected Proton NMR Spectral Data[a]

complex	assignt	δ,[b] ppm		coupling, Hz		complex	assignt	δ,[b] ppm		coupling, Hz	
3	Rh*H*	−7.72	ddt	$J(HP_{trans})$	171.1	**14**	Rh*H*	−9.00	dpqu	$J(HP_{trans})$	156.3
				$J(HP_{cis})$	8.9					$J(HP_{cis})$	12.1
				J(HRh)	15.5					J(HRh)	12.1
	C≡*CH*	2.31	pqu	^3J(HRh)	2.1		C≡CC_6H_5	*c*			
				^4J(HP)	2.1	**15**	Rh*H*	−9.09	dpqu	$J(HP_{trans})$	155.3
4	Rh*H*	−7.79	ddt	$J(HP_{trans})$	172.2					$J(HP_{cis})$	13.4
				$J(HP_{cis})$	9.5					J(HRh)	13.4
				J(HRh)	15.6		C≡C*Si*Me_3	0.32	s		
	CH_2CH_2CH_3	2.55	tqd	J(HH)	6.9	**16**	Rh*H*	−9.14	dpqu	$J(HP_{trans})$	157.3
				^5J(HP)	2.1					$J(HP_{cis})$	12.2
				^4J(HRh)	0.7					J(HRh)	12.2
	CH_2*C*H_2CH_3	1.71	psexq	J(HH)	7.1		*C*H_2OH	4.58	dm	J(HH)	6.0
				^6J(HP)	1.0		CH_2*O*H	3.76	t		
	CH_2CH_2*C*H_3	1.16	t			**17**	Rh*H*	−9.12	dpqu	$J(HP_{trans})$	156.3
5	Rh*H*	−7.61	ddt	$J(HP_{trans})$	171.2					$J(HP_{cis})$	13.1
				$J(HP_{cis})$	8.9					J(HRh)	13.1
				J(HRh)	15.8		*C*HO	8.17	m		
	C≡CC_6H_5	*c*				**18**	Rh*H*	−9.24	dpqu	$J(HP_{trans})$	151.3
6	Rh*H*	−7.58	ddt	$J(HP_{trans})$	170.7					$J(HP_{cis})$	11.7
				$J(HP_{cis})$	9.3					J(HRh)	11.7
				J(HRh)	15.9		COO*H*	*d*			
	C≡C*Si*Me_3	0.29	s			**19**	Rh*H*	−9.06	dpqu	$J(HP_{trans})$	152.8
7	Rh*H*	−7.78	ddt	$J(HP_{trans})$	172.4					$J(HP_{cis})$	11.8
				$J(HP_{cis})$	9.1					J(HRh)	11.8
				J(HRh)	15.6		O*C*H_2CH_3	4.24	q	J(HH)	7.5
	CH_2OH	4.52	dm	J(HH)	5.9		OCH_2*C*H_3	1.35	t		
	CH_2*O*H	3.81	brt			**20**[f]	C≡*CH*	5.32	m		
8	RhH	−7.13	ddt	$J(HP_{trans})$	150.3		O*C*H_2CH_3	4.00	q	J(HH)	8.2
				$J(HP_{cis})$	5.7		OCH_2*C*H_3	1.24	t		
				J(HRh)	16.0	**21**[f]	C≡*CH*	6.48	m		
	*C*HO	8.02	m				O*C*H_2CH_3	3.89	q	J(HH)	8.0
9	Rh*H*	−7.58	ddt	$J(HP_{trans})$	169.3		OCH_2*C*H_3	1.21	t		
				$J(HP_{cis})$	8.4	**22**[g]	*C*H_2CH_2CH_3	2.62	tq	J(HH)	7.1
				J(HRh)	15.4					^5J(HP)	2.8
	O*C*H_2CH_3	4.20	q	J(HH)	7.1		CH_2*C*H_2CH_3	1.67	psex	J(HH)	7.1
	OCH_2*C*H_3	1.32	t				CH_2CH_2*C*H_3	1.05	t		
10	Rh*H*	−7.59	ddt	$J(HP_{trans})$	169.0	**23**[g]	C≡CC_6H_5	*c*			
				$J(HP_{cis})$	7.8	**24**	C≡C*Si*Me_3	0.05	s		
				J(HRh)	15.5	**25**[g]	*C*H_2OH	4.29	dq	J(HH)	5.2
	COO*H*	9.81	brm							^5J(HP)	2.8
11	Rh*H*	−7.09	ddt	$J(HP_{trans})$	193.3		CH_2*O*H	1.02	t		
				$J(HP_{cis})$	5.7	**26**	O*C*H_2CH_3	4.09	q	J(HH)	7.0
				J(HRh)	11.6		OCH_2*C*H_3	1.28	t		
	C≡*CH*	d				**27**[g]	*C*H_2CH_2CH_3	2.45	tq	J(HH)	7.2
12	Rh*H*	−9.12	dpqu	$J(HP_{trans})$	156.9					^5J(HP)	2.5
				$J(HP_{cis})$	12.2		CH_2*C*H_2CH_3	1.57	psex	J(HH)	7.2
				J(HRh)	12.2		CH_2CH_2*C*H_3	0.97	t		
	C≡*CH*	2.54	brm			**28**[g]	C≡CC_6H_5	*c*			
13	Rh*H*	−9.15	dpqu	$J(HP_{trans})$	157.8	**29**[g]	C≡C*Si*Me_3	0.39	s		
				$J(HP_{cis})$	13.1	**30**	*C*H_2OH	4.34	dq	J(HH)	5.2
				J(HRh)	13.1		CH_2*O*H	1.08	t		
	CH_2CH_2CH_3	*e*				**31**[h]	*C*HO	9.04	q	^5J(HP)	1.1
	CH_2*C*H_2CH_3	1.76	psex	J(HH)	7.1	**32**[g]	O*C*H_2CH_3	4.04	q	J(HH)	7.1
	CH_2CH_2*C*H_3	1.19	t				OCH_2*C*H_3	1.15	t		

[a] At room temperature in acetone-d_6 solution unless otherwise stated. [b] In ppm from external TMS. The resonances due to the hydrogen atoms of the tripodal ligands are not reported. Key: s, singlet; d, doublet; t, triplet; q, quartet; pqu, pseudoquintuplet; psex, pseudosextuplet; m, multiplet; br, broad. [c] Masked by the aromatic protons of the ligand and of the tetraphenylborate anion. [d] Not located. [e] Obscured by the aliphatic protons of the PP_3 ligand in the 2.5–3.0 ppm region. [f] At 233 K in THF-d_8 solution. [g] At room temperature in C_6D_6 solution. [h] At room temperature in CD_2Cl_2 solution.

A summary of crystal and intensity data is reported in Table V. All X-ray measurements were performed on a Philips PW1100 automated four-circle diffractometer with a Mo Kα radiation monochromatized with a graphite crystal. The cell parameters were determined by least-squares refinement of the setting angles of 25 carefully centered reflections. As a general procedure, three standard reflections were collected every 2 h (no decay of intensities was observed in any case). Intensity data were corrected for Lorentz–polarization effects. Atomic scattering factors were those reported by Cromer and Waber[9] with anomalous dispersion corrections taken from ref 10. All the calculations were done on a SEL 32/77 computer, installed in our Institute, by using SHELX 76 program.[11] The structure was solved by Patterson and Fourier techniques. Refinement was done by full-matrix least-squares calculations initially with isotropic thermal parameters. Anisotropic thermal parameters were used only for the Rh and P atoms. The phenyl rings were treated as rigid bodies of D_{6h} symmetry with C–C distances fixed at 1.395 Å and calculated hydrogen atom positions (C–H = 0.96 Å). The hydrogen atom bound to rhodium was found from a difference Fourier map, and its positional and isotropic thermal parameters were refined. None of the residual peaks detected in the Fourier difference map allows to localize the ethynyl hydrogen ligand. A difference map showed

(9) Cromer, D. T.; Waber, J. T. *Acta Crystallogr.* **1965**, *18*, 104.
(10) *International Tables of Crystallography*; Kynoch: Birmingham, England, 1974; Vol. 4.
(11) Sheldrick, G. M. SHELX76, Program for Crystal Structure Determination; University of Cambridge: Cambridge, England, 1976.

Table IV. $^{31}P\{^1H\}$ NMR Data for the Complexes[a]

complex	pattern	δ(P),[b] ppm		coupling, Hz J(PP)		coupling, Hz J(PRh)
3	AM_2X	P_A	18.51	19.7	P_ARh	86.2
		P_M	34.69		P_MRh	103.9
4	AM_2X	P_A	18.33	19.8	P_ARh	86.4
		P_M	34.08		P_MRh	104.2
5	AM_2X	P_A	19.98	19.7	P_ARh	86.0
		P_M	35.57		P_MRh	102.4
6	AM_2X	P_A	18.51	20.0	P_ARh	86.2
		P_M	33.67		P_MRh	102.6
7	AM_2X	P_A	17.71	19.5	P_ARh	85.8
		P_M	34.34		P_MRh	103.4
8	AM_2X	P_A	23.11	19.3	P_ARh	92.1
		P_M	37.01		P_MRh	100.4
9	AM_2X	P_A	20.19	19.1	P_ARh	84.0
		P_M	36.69		P_MRh	100.9
10	AM_2X	P_A	26.79	19.9	P_ARh	90.2
		P_M	39.92		P_MRh	106.3
11	AM_2X	P_A	25.61	33.8	P_ARh	102.7
		P_M	28.72		P_MRh	133.7
12	AM_2QX[b]	P_A	134.81	P_AP_M 9.3	P_ARh	74.6
		P_M	43.76	P_AP_Q 9.3	P_MRh	97.5
		P_Q	36.39	P_MP_Q 17.5	P_QRh	83.2
13	AM_2QX	P_A	134.38	P_AP_M 8.9	P_ARh	74.9
		P_M	43.24	P_AP_Q 8.9	P_MRh	98.1
		P_Q	36.00	P_MP_Q 17.4	P_QRh	83.1
14	AM_2QX	P_A	134.58	P_AP_M 8.8	P_ARh	74.9
		P_M	44.16	P_AP_Q 8.8	P_MRh	96.8
		P_Q	36.87	P_MP_Q 17.5	P_QRh	83.0
15	AM_2QX	P_A	134.06	P_AP_M 8.9	P_ARh	73.7
		P_M	42.62	P_AP_Q 8.9	P_MRh	96.8
		P_Q	36.62	P_MP_Q 17.7	P_QRh	83.7
16	AM_2QX	P_A	134.31	P_AP_M 9.4	P_ARh	74.9
		P_M	43.54	P_AP_Q 9.4	P_MRh	98.1
		P_Q	35.48	P_MP_Q 17.6	P_QRh	82.9
17	AM_2QX	P_A	134.55	P_AP_M 8.7	P_ARh	74.9
		P_M	43.92	P_AP_Q 9.3	P_MRh	97.1
		P_Q	36.77	P_MP_Q 17.5	P_QRh	82.9
18	AM_2QX	P_A	134.30	P_AP_M 9.3	P_ARh	75.7
		P_M	46.03	P_AP_Q 9.3	P_MRh	95.1
		P_Q	37.00	P_MP_Q 17.6	P_QRh	82.9
19	AM_2QX	P_A	136.47	P_AP_M 8.6	P_ARh	74.6
		P_M	45.88	P_AP_Q 8.6	P_MRh	95.8
		P_Q	38.75	P_MP_Q 17.1	P_QRh	83.0
20[c]	A_3X	P_A	27.17		P_ARh	110.9
21[c]	AM_3X	P_A	141.60	P_AP_M 10.1	P_ARh	101.6
		P_M	54.53		P_MRh	135.7
22[e]	A_3X	P_A	23.37		P_ARh	183.8
23	A_3X	P_A	24.68		P_ARh	160.7
24	A_3X	P_A	23.18		P_ARh	162.7
25[d]	A_3X	P_A	24.56		P_ARh	160.5
26	A_3X	P_A	25.95		P_ARh	157.5
27[d]	AM_3X	P_A	153.25	P_AP_M 21.5	P_ARh	89.5
		P_M	47.31		P_MRh	151.4
28	AM_3X	P_A	151.58	P_AP_M 21.7	P_ARh	87.6
		P_M	46.66		P_MRh	149.8
29[d]	AM_3X	P_A	151.49	P_AP_M 21.2	P_ARh	86.6
		P_M	45.78		P_MRh	151.0
30	AM_3X	P_A	152.04	P_AP_M 21.9	P_ARh	88.8
		P_M	46.92		P_MRh	149.7
31	AM_3X	P_A	151.13	P_AP_M 22.8	P_ARh	86.7
		P_M	49.97		P_MRh	147.3
32[d]	AM_3X	P_A	150.15	P_AP_M 22.5	P_ARh	87.5
		P_M	48.10		P_MRh	148.3

[a] Chemical shifts (δ) are relative to 85% H_3PO_4 with positive values being downfield from the standard. All the spectra were recorded in acetone-d_6 at room temperature unless otherwise stated. [b] In the PP_3 complexes, P_A denotes the bridgehead phosphorus atom, while P_M and P_Q denote the terminal phosphorus donors. [c] Recorded at 233 K. [d] Benzene-d_6 as solvent.

some relatively high peaks that were assigned to THF solvent molecules. From proton NMR spectroscopy and elemental analysis the stoichiometric ratio between the rhodium complex and THF solvent molecules was found to be 1:1.5. Since the thermal parameters relative to tetrahydrofuran refined to an acceptable value by assuming an atomic population parameter of 1.5, the ratio given above was confirmed to be correct.

Atomic coordinates for all the non-hydrogen atoms are given in Tables S1 and S2.

Table V. Summary of X-ray Diffraction Data for $[(NP_3)Rh(H)(C{\equiv}CH)]BPh_4 \cdot 1.5\ C_4H_8O$

formula	$C_{74}H_{76}B_1N_1O_{1.5}P_3Rh_1$
fw	1210.07
cryst system	monoclinic
space group	$P2_1/n$ (No. 14)
a, Å	15.769 (3)
b, Å	32.458 (6)
c, Å	13.277 (3)
β, deg	105.21 (2)
V, Å^3	6557.52
Z	4
D(calcd), g cm^{-3}	1.225
cryst dimen, mm	0.67 × 0.17 × 0.16
μ(Mo Kα), cm^{-1}	3.19
radiatn	Mo K_α (0.710 69 Å, graphite monochromator)
scan type	ω–2θ
2θ range, deg	5–50
scan width	0.9
scan speed, deg s^{-1}	0.04
total data	12319
no. of unique obsd data, $I > 3\sigma(I)$	3735
no. of parameters	279
R	0.079
R_w	0.086
abs correctn	DIFABS
transmissn factors, max, min	0.98, 0.91

Results

Reactivity of the 16-Electron Fragments $[(NP_3)Rh]^+$ and $[(PP_3)Rh]^+$ with 1-Alkynes. The trigonal-bipyramidal (TBP) hydrides $[(NP_3)RhH]$ (1) and $[(PP_3)RhH]$ (2) in THF undergo electrophilic attack by CH_3^+ from $MeOSO_2CF_3$ to produce, following the elimination of methane, coordinatively and electronically unsaturated fragments that are appropriately designed to oxidatively add C–H bonds.[5,12] In reality, the NP_3 hydride primarily yields the ortho-metalated complex $[\{(Ph_2PCH_2CH_2)_2N(CH_2CH_2PPhC_6H_4)\}RhH]BPh_4$ (Scheme II). This, however, readily undergoes the reductive elimination of the metalated phenyl, thus virtually forming the 16-electron fragment $[(NP_3)Rh]^+$, by reaction with various substrates.[5,12] We now show that also terminal alkynes with a very few exceptions promote the phenyl reductive elimination. Ultimately, both the $[(NP_3)Rh]^+$ system and its congener $[(PP_3)Rh]^+$ react with 1-alkynes to give products whose nature is strictly dependent on that of the alkyne substituent and the reaction conditions as well.

Room-Temperature Reactions. At room temperature, $[(NP_3)Rh]^+$, prepared in situ, reacts with the terminal alkynes reported in Scheme II to give cis hydride acetylide complexes of rhodium(III) regardless of the nature of the substituent except $BrCH_2C{\equiv}CH$. In this case, in fact, the ortho-metalated form of the NP_3 system is stabilized via H–Br metathesis, thus impeding any further interaction of the metal with the C–C triple bond.[5] Cis hydride acetylides are obtained also by reacting the $[(PP_3)Rh]^+$ fragment with 1-alkynes (Scheme II). All of the compounds are colorless to fairly yellow crystalline solids that

(12) (a) Bianchini, C.; Meli, A.; Peruzzini, F.; Zanobini, F. *J. Chem. Soc., Chem. Commun.* **1987**, 971. (b) Bianchini, C.; Meli, A.; Peruzzini, M.; Vacca, A.; Zanobini, F. *Organometallics* **1987**, *6*, 2453. (c) Bianchini, C.; Peruzzini, M.; Vizza, F.; Zanobini, F. *J. Organomet. Chem.* **1988**, *348*, C9. (d) Bianchini, C.; Meli, A.; Peruzzini, M.; Ramirez, A. J.; Vacca, A.; Vizza, F.; Zanobini, F. *Organometallics*, in press.

Scheme II

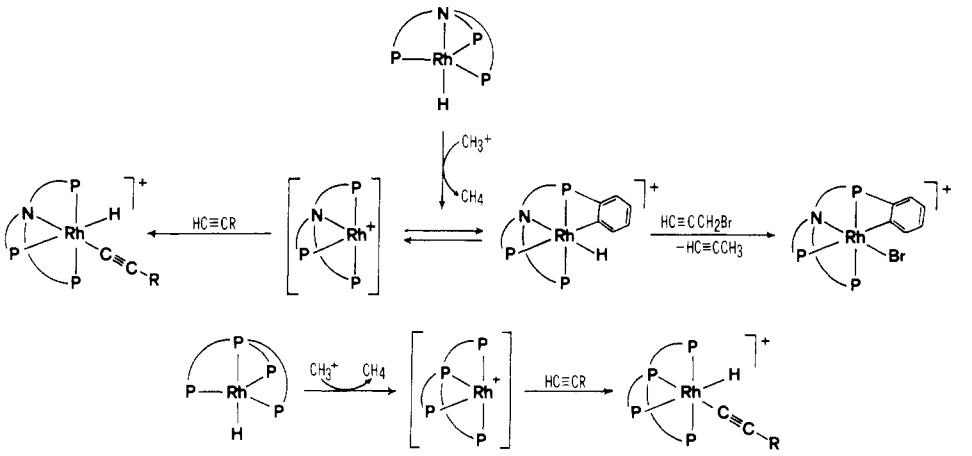

R = H, n-C_3H_7, Ph, $SiMe_3$, CH_2OH, CHO, CO_2H, CO_2Et

were isolated as BPh_4^- salts of formula $[(L)Rh(H)(C{\equiv}CR)]BPh_4$ [L = NP_3, R = H (**3**), n-C_3H_7 (**4**), Ph (**5**), $SiMe_3$ (**6**), CH_2OH (**7**), CHO (**8**), CO_2Et (**9**), CO_2H (**10**); L = PP_3, R = H (**12**), n-C_3H_7 (**13**), Ph (**14**), $SiMe_3$ (**15**), CH_2OH (**16**), CHO (**17**), CO_2H (**18**), CO_2Et (**19**)]. They all are air-stable both in the solid state and in solution in which they behave as 1:1 electrolytes (see Table I). The IR spectra contain weak bands, ranging from 2050 to 1970 cm^{-1}, which are assigned to ν(Rh–H). Each Rh–H stretching band is accompanied by a strong absorption at higher frequency in the region of σ-bonded acetylide ligands (between 2120 and 2010 cm^{-1} except for the two ethynyl ligands in complexes **3** and **12** which exhibit a lower energy absorption).[1] When the acetylide ligands bear substituents that have characteristic IR absorptions, these are obviously observed and can be safely used as diagnostic tools for structural assignments. As an example, the bands due to the carbonyl group in the propynyl derivatives with CHO, CO_2H, or CO_2Et substituents indicate that the functional groups are in the intact form. All of the most significative absorptions in the IR spectra are reported in Tale I together with a list of ν(Rh—H) and ν(C≡C) vibrations. Finally, the typical band at ca. 610 cm^{-1} as well as the phenyl-reinforced vibration at 1580 cm^{-1} diagnoses the presence of the tetraphenylborate counterion.

The $^{31}P\{^1H\}$ NMR spectra of the NP_3 complexes **3–9** (Table IV) invariably show first-order AM_2X splitting patterns consistent with octahedral (OCT) geometries in which the $[(NP_3)Rh]^+$ fragment is arranged in the butterfly shape (C_{2v} symmetry) (I).[5,12]

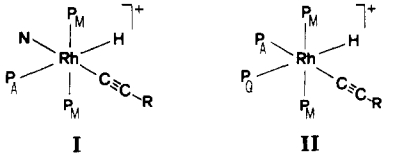

I II

The resonance due to the two equivalent, mutually trans phosphorus atoms, P_M, appears as doublets of doublets (dd) due to coupling to rhodium and to the equatorial phosphorus atom P_A. The signals of the latter nucleus, consisting of doublets of triplets (dt), is invariably located at higher fields with respect to P_M because of the trans influence of the hydride ligand (vide infra). The steric requirements of the tripodal polyphosphine are clearly put in evidence by the ^{31}P NMR data which are consistent with OCT geometries in which the hydride and acetylide ligands are mutually cis. Interestingly, the oxidative addition of the sp C–H bonds at rhodium occurs in a highly stereospecific manner as the hydride ligand is invariably located trans to the equatorial phosphorus atom P_A rather than to the nitrogen. This assignment is unequivocally demonstrated by proton NMR measurements which show, in the high-field region of the spectra, two well-resolved doublets of triplets (see Table III) for the hydride hydrogen atoms. The J(HP) values that are responsible for the observed halving of the signals (150.3–172.4 Hz) are typical of $H–P_{trans}$ coupling.[5,12] The experimental and computed spectra for the hydride resonances of two representative compounds, namely, $[(NP_3)Rh(H)(C{\equiv}CSiMe_3)]BPh_4$ (**6**) and $[(PP_3)Rh(H)(C{\equiv}CSiMe_3)]BPh_4$ (**15**), are reported in Figure 1.

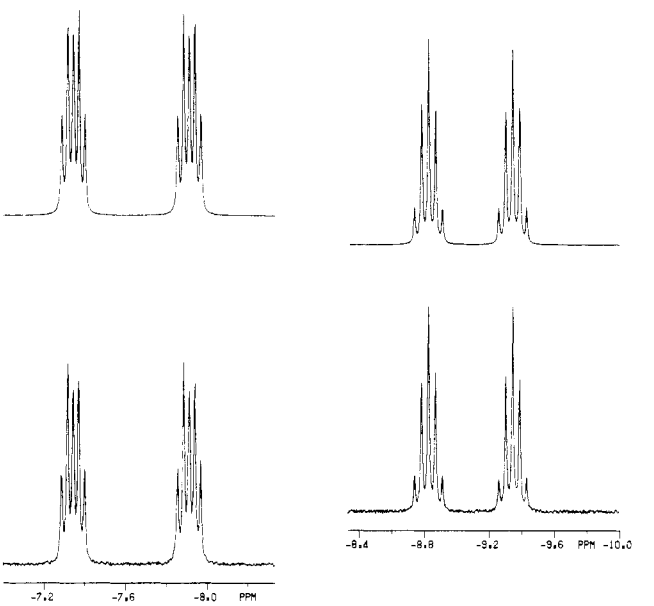

Figure 1. Experimental (bottom) and computed (top) ^1H NMR spectra (300 MHz, 298 K, CD_3COCD_3, TMS reference) in the hydride region of **6** (a) and **15** (b).

By using the same spectroscopic criterion, OCT geometries (II) are assigned also to the PP_3 derivatives **12–19** (Table IV).[5,12] Indeed, all of these complexes exhibit first-order AM_2QX splitting patterns consisting of three well-separated resonances of intensity ratio 1:2:1. Each resonance is obviously doubled by coupling to ^{103}Rh. The low-field signal, consisting of a doublet of pseudoquartets, is assigned to the bridgehead phosphorus atom of the PP_3 ligand which lies in the equatorial plane of the octahedron. The high value of the coordination chemical shift [$\Delta(P)$

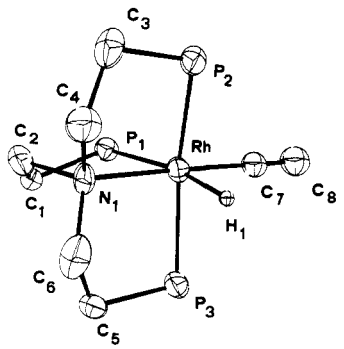

Figure 2. ORTEP drawing of the $[(NP_3)Rh(H)(C{\equiv}CH)]^+$ complex cation. Hydrogen atoms of the ethylenic chains and phenyl rings of the NP_3 ligand are omitted for clarity.

$= \delta(P_{coord}) - \delta(P_{free\ ligand}) \geq 146$ ppm] is due to the fact that the central phosphorus is involved in three five-membered metallaring systems.[13] Finally, the presence of a doublet of pseudoquartets is originated by identical coupling of P_A to the three cis phosphorus nuclei [i.e. $J(P_AP_M) \cong J(P_AP_Q)$] as confirmed by P–P decoupling experiments. The most intense resonance, which appears as a doublet of doublets of doublets, is assigned to the two equivalent P_M phosphorus atoms lying trans to each other in the axial positions of the coordination polyhedron. In conclusion, the third signal, which is invariably the highest field resonance present in all these spectra, can be assigned to the remaining terminal phosphorus atom P_Q. Such a resonance appears as a doublet of triplets of doublets owing to different coupling to the two axial P_M atoms and to the central P_A nucleus. As we and other authors have previously observed, the coupling connection involving different types of terminal phosphorus atoms in tripodal polyphosphines gives results larger than those involving the central P donor.[5,14]

The ^1H NMR spectra of compounds **12–19** are characterized by the presence of doublets of pseudoquintuplets in the high-field region that are assigned to the hydride resonances. Figure 1b reports the observed and computed spectrum for the *cis* (trimethylsilyl)acetylide hydride complex **15** in the hydride region. This multiplicity is originated by strong coupling to a trans phosphorus atom [$J(HP_{trans}) \geq 151$ Hz] and by additional coupling to the three terminal phosphorus atoms of the PP_3 ligand and to rhodium. The former, although nonequivalent, exhibits casual coincidence to the coupling constants to the hydride, which, furthermore, is equally coupled to the rhodium atom. The fortuitous coincidence of these three coupling constants [$J(P_MH) \cong J(P_QH) \cong J(RhH)$] is responsible for the observed pseudoquintets and has some precedents in rhodium hydride complexes with polyphosphine ligands.[5,15] As expected, proton-coupled ^{31}P NMR spectroscopy allows us to establish the position of the hydride ligand as lying trans to the terminal equatorial P_Q atom rather than to the bridgehead phosphorus atom P_A, which in turn is located trans to the alkynyl ligand in the equatorial plane of the octahedron (II).

In order to confirm the stereospecific addition of 1-alkynes to the $[(L)Rh]^+$ fragments (L = NP_3, PP_3) as well as to obtaine crystallographic data for this class of novel compounds, we carried out an X-ray diffraction study on **3**·1.5THF, which is the first authenticated cis ethynyl hydride metal complex.

Table VI. Selected Bond Distances (Å) and Angles (deg) for $[(NP_3)Rh(H)(C{\equiv}CH)]BPh_4 \cdot 1.5\ C_4H_8O$

Bond Distances			
Rh(1)–H(1)	1.4 (1)	P(3)–C(5)	1.84 (2)
Rh(1)–P(1)	2.382 (4)	N(1)–C(2)	1.49 (2)
Rh(1)–P(2)	2.305 (4)	N(1)–C(4)	1.52 (2)
Rh(1)–P(3)	2.312 (4)	N(1)–C(6)	1.52 (2)
Rh(1)–N(1)	2.17 (1)	C(1)–C(2)	1.54 (2)
Rh(1)–C(7)	1.96 (1)	C(3)–C(4)	1.51 (3)
P(1)–C(1)	1.86 (1)	C(5)–C(6)	1.45 (2)
P(2)–C(3)	1.82 (1)	C(7)–C(8)	1.20 (2)
Bond Angles			
N(1)–Rh(1)–C(7)	178.2 (5)	Rh(1)–P(2)–C(3)	100.0 (6)
P(1)–Rh(1)–C(7)	96.7 (4)	Rh(1)–P(3)–C(5)	100.5 (5)
P(1)–Rh(1)–N(1)	84.2 (3)	Rh(1)–N(1)–C(2)	115.2 (8)
P(1)–Rh(1)–P(2)	102.9 (1)	Rh(1)–N(1)–C(6)	110.0 (8)
P(1)–Rh(1)–P(3)	100.4 (1)	Rh(1)–N(1)–C(4)	108.7 (9)
P(2)–Rh(1)–C(7)	95.1 (4)	C(2)–N(1)–C(6)	110 (1)
P(2)–Rh(1)–N(1)	86.3 (3)	C(2)–N(1)–C(4)	105 (1)
P(2)–Rh(1)–P(3)	153.9 (1)	C(4)–N(1)–C(6)	108 (1)
P(3)–Rh(1)–C(7)	93.5 (4)	P(1)–C(1)–C(2)	108.6 (9)
P(3)–Rh(1)–N(1)	84.8 (3)	N(1)–C(2)–C(1)	113 (1)
H(1)–Rh(1)–C(7)	83 (4)	P(3)–C(5)–C(6)	109 (1)
H(1)–Rh(1)–N(1)	96 (4)	N(1)–C(6)–C(5)	114 (1)
H(1)–Rh(1)–P(1)	168 (5)	P(2)–C(3)–C(4)	110 (1)
H(1)–Rh(1)–P(2)	89 (5)	N(1)–C(4)–C(3)	113 (1)
H(1)–Rh(1)–P(3)	68 (5)	Rh(1)–C(7)–C(8)	177 (1)
Rh(1)–P(1)–C(1)	98.8 (5)		

The ORTEP drawing of the complex cation is shown in Figure 2. Selected bond angles and distances are reported in Table VI. The structure consists of discrete mononuclear $[(NP_3)Rh(H)(C{\equiv}CH)]^+$ cations, BPh_4^- anions, and solvate THF molecules in the stoichiometric ratio of 1:1:1.5. In keeping with the chemical-physical characterization of the complex, the rhodium center is coordinated in a slightly distorted OCT arrangement by the four donor atoms of the NP_3 ligand, the hydride, and the σ-ethynyl ligand. As expected, the acetylide group lies trans to nitrogen and cis to the hydridic hydrogen atom. The Rh–C(7)–C(8) moiety is virtually linear [177 (1)°] in nice agreement with previously reported data on X-ray authenticated σ-alkynyl complexes.[3c,16] The hydride ligand exerts the highest trans influence, the Rh–P(1) bond [2.382 (4) Å] being the longest of the three [Rh–P(2) = 2.305 (4), Rh–P(3) = 2.316 (4) Å]. The two mutually trans PPh_2 groups are significatively bent over the plane defined by Rh, H(1), and C(7), with the angle P(2)–Rh–P(3) equal to 153.9 (1)°. The butterfly shape of the $[(NP_3)Rh]^+$ fragment has been previously found in other OCT complexes such as the carbon disulfide adduct $[(NP_3)Rh(\eta^2\text{-}CS_2)]BPh_4$[17] and the ortho-metalated derivative $[\{(Ph_2PCH_2CH_2)_2N(CH_2CH_2PPhC_6H_4)\}RhI]$-$BPh_4$.[5] The Rh–C(7) bond distance [1.96 (1) Å] matches the expected value for a single bond, Rh–C(sp). Also, the C(7)–C(8) bond distance [1.20 (2) Å] falls in the range that is expected for terminal alkynyl ligands.[3c,16] This fact and the high-energy value of the IR stretching absorption of the C–C triple bond [$\nu(C{\equiv}C) = 1975\ cm^{-1}$] suggest a scarce π-back-donation from rhodium to π^*-orbitals of the ethynyl moiety.[3c] Finally, the Rh–H(1) bond distance [1.4 (1)

(13) Garrou, P. E. *Chem. Rev.* **1981**, *81*, 229.
(14) (a) Hohman, W. H.; Kountz, D. J.; Meek, D. W. *Inorg. Chem.* **1986**, *25*, 616. (b) Du Bois, D. L.; Miedaner, A. *Ibid.* **1986**, *25*, 4642.
(15) (a) Slack, D. A.; Greveling, J.; Baird, M. C. *J. Am. Chem. Soc.* **1979**, *101*, 3125. (b) Di Vaira, M.; Peruzzini, M.; Zanobini, F.; Stoppioni, P. *Inorg. Chim. Acta* **1983**, *69*, 37.
(16) (a) Nast, R. *Coord. Chem. Rev.* **1982**, *47*, 89. (b) Furlani, A.; Licoccia, S.; Russo, M. V.; Chiesi Villa, A.; Guastini, C. *J. Chem. Soc., Dalton Trans.* **1982**, 2449. (c) Furlani, A.; Licoccia, S.; Russo, M. V.; Chiesi Villa, A.; Guastini, C. *Ibid.* **1984**, 2197. (d) Buang, N. A.; Hughes, D. L.; Kashef, N.; Richards, R. L.; Pombeiro, A. J. L. *J. Organomet. Chem.* **1987**, *323*, C47. (e) Hills, A.; Hughes, D. L.; Kashef, N.; Richards, R. L.; Lemos, M. A.; Pombeiro, A. J. L. *Ibid.* **1988**, *350*, C4.
(17) Bianchini, C.; Masi, D.; Mealli, C.; Meli, A.; Sabat, M. *Organometallics* **1985**, *4*, 1014.

Å] is in line with many other Rh(III)–hydride distances previously reported.[18]

Low-Temperature Reactions. Decreasing the temperature does not change the nature of the products of the reactions of $[(NP_3)Rh]^+$ and $[(PP_3)Rh]^+$ with 1-alkynes except for ethyl propiolate, $HC{\equiv}CCO_2Et$, and propiolic acid, $HC{\equiv}CCO_2H$.

The $HC{\equiv}CCO_2Et$ Case. Both metal fragments react with $HC{\equiv}CCO_2Et$ in THF at −40 °C to give orange (NP_3) or yellow (PP_3) solutions exhibiting ^{31}P NMR spectra quite different from those recorded at room temperature. Addition of petroleum ether or *n*-hexane to the cold reaction mixtures precipitates orange or yellow-green microcrystals of $[(NP_3)Rh(\pi\text{-}HC{\equiv}CCO_2Et)](SO_3CF_3)$ (**20**) and $[(PP_3)Rh(\pi\text{-}HC{\equiv}CCO_2Et)](SO_3CF_3)$ (**21**) which maintain the spectroscopic properties of the solution products. Both compounds are moderately air-stable in the solid state and remain unchanged in low-temperature deoxygenated solutions in which they behave as 1:1 electrolytes. The presence of a η^2-bonded ethyl propiolate molecule is clearly shown by the IR spectra which do not contain absorptions in the σ-acetylide or terminal hydride stretching regions. In contrast, strong absorptions at ca. 1780 cm^{-1} are consistent with the presence of a π-bonded alkyne ligand which behaves midway between a two- and four electron donor.[19] Moreover, the proton NMR spectra of **20** and **21**, recorded at −40 °C in THF-d_8, contain no signal in the hydride region but show multiplets (1 H) at 5.32 and 6.48 ppm, respectively, which can be assigned to the alkyne C–H protons.[1]

The insertion of metal species across C–H bonds from alkynes is predicted to be favored at high temperature.[20] As a matter of fact, heating solutions of **20** or **21** promotes the insertion of rhodium across the C–H bond of ethyl propiolate to give quantitatively the Rh(III) cis hydride acetylide complexes **9** and **19**.

The π-alkyne → cis hydride acetylide conversion can be monitored by $^{31}P\{^1H\}$ NMR spectroscopy. In particular, increasing the temperature of a sample of 30 mg of the NP_3 derivative **20** in 3 mL of THF-d_8 from −40 to 0 °C makes the AM_2X spin system [$\delta(P_A)$ = 20.99 ppm, $\delta(P_M)$ = 33.67 ppm; $J(PP)$ = 27.9, $J(P_ARh)$ = 85.2, $J(P_MRh)$ = 102.5 Hz] collapse into a broad signal which becomes a sharp doublet at 25 °C [A_3X pattern; δ = 27.17 ppm; $J(PRh)$ = 110.9 Hz]. Maintaining the sample at the latter temperature results in the progressive disappearance of the doublet and contemporaneous appearance of the AM_2X pattern of the cis hydride acetylide **9**. The conversion is completed in 10 min. In a similar way, the PP_3 derivative **21**, which exhibits a ^{31}P NMR AM_3X pattern over the temperature range −70 to 0 °C [$\delta(P_A)$ = 141.60 ppm, $\delta(P_M)$ = 54.53 ppm; $J(PP)$ = 10.1, $J(P_ARh)$ = 101.6, $J(P_MRh)$ = 111.5 Hz], completely converts into the cis hydride acetylide **19** (AM_2QX spin system) on standing at 0 °C for ca. 15 min. The conversion is much faster at higher temperature (ca. 5 min at 20 °C). When the temperature of a solution of **21** in THF is lowered from −70 to −90 °C, the M_3 portion of the AM_3X spectrum collapses into two 1:2 poorly resolved signals [$\delta(P_Q) \cong 57.5$, $\delta(P_M) \cong 53.0$ ppm], indicating that the limiting pattern is most likely AM_2QX also for **21**. Figure 3 shows the $^{31}P\{^1H\}$ NMR spectra of a solution of 30 mg of **21** in 3 mL of THF-d_8 at −40 °C and after standing at +20 °C for 5 min.

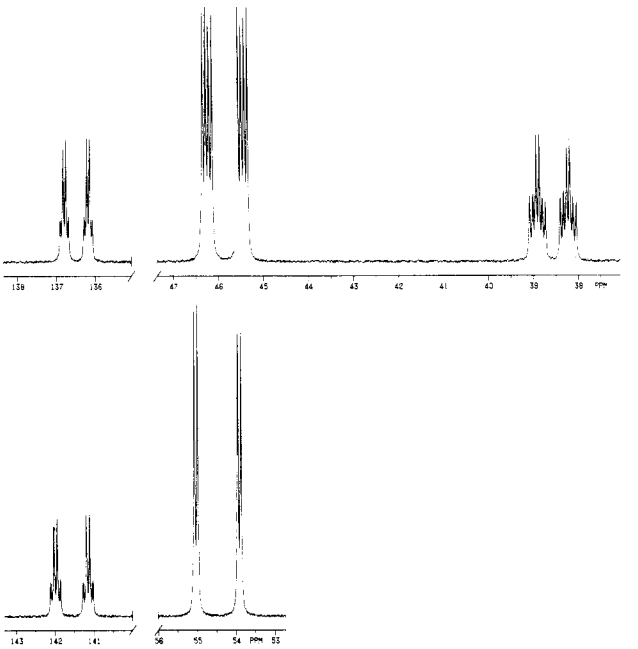

Figure 3. $^{31}P\{^1H\}$ NMR spectrum of **21** in THF-d_8 at 233 K (bottom) and at 293 K (top).

Interestingly, while in both cases, the low-temperature exchange $AM_2QX \rightleftarrows AM_3X$ (**21**) or $AM_2X \rightleftarrows A_3X$ (**20**) is reversible and controlled by the temperature, thus indicating fluxionality, the high-temperature exchange $AM_3X \rightarrow AM_2QX$ (**21**) or $A_3X \rightarrow AM_2X$ (**20**) is irreversible. In fact, decreasing the temperature of THF solutions of **9** or **19** down to −100 °C does not change the ^{31}P NMR spectrum; i.e., the regeneration of the π-alkyne complexes via intramolecular reductive elimination of the alkyne sp C–H bond at rhodium does not occur. In other words, the OCT complexes **9** and **19** appear as the thermodynamic products that are irreversibly formed when the kinetic barrier is overridden.

The $HC{\equiv}CCO_2H$ Case. The reactions of propiolic acid with the 16-electron fragments $[(NP_3)Rh]^+$ and $[(PP_3)Rh]^+$ are separately discussed because of the particular results obtained. We looked at this alkynoic acid as it contains a highly acidic proton which, in principle, may compete with the alkyne proton in undergoining oxidative addition at rhodium. In effect, it has recently been reported for some rhodium(I) and iridium(I) complexes that the oxidative cleavage of the carboxylic O–H bond may prevail over that of the alkyne C–H bond.[3]

Interestingly, while $[(PP_3)Rh]^+$ and $HC{\equiv}CCO_2H$ in THF give the expected OCT cis hydrido acetylide complex **18** with no trace of alternative O–H carboxylic activation, the reaction of the $[(NP_3)Rh]^+$ fragment proceeds through a less discriminating path. Monitoring the reaction by $^{31}P\{^1H\}$ and ^1H NMR spectroscopies reveals that the initial interaction of the alkyne with the metal system is of the π-type. In particular, the proton NMR spectrum recorded at −40 °C in acetone-d_6 or THF-d_8 initially contains no signal in the hydride region, while the $^{31}P\{^1H\}$ NMR

(18) (a) Yoshida, T.; Thorn, D. L.; Okano, T.; Ibers, J. A.; Otsuka, S. *J. Am. Chem. Soc.* **1979**, *101*, 4212. (b) Muir, K. W.; Ibers, J. A. *Inorg. Chem.* **1970**, *9*, 440. (c) Geerts, L. R.; Huffman, J. C.; Wersterberg, D. E.; Folting, K.; Caulton, K. G. *New. J. Chem.* **1988**, *12*, 455. (d) Ott, J.; Venanzi, L. M.; Ghilardi, C. A.; Midollini, S.; Orlandini, A. *J. Organomet. Chem.* **1985**, *291*, 89.

(19) (a) Collmann, J. P.; Hegedus, L. S. *Principles and Applications of Organotransition Metal Chemistry*; University Science Book: Mill Valley, CA, 1980. (b) Shur, V. B.; Burlakov, V. V.; Vol'pin, M. E. *J. Organomet. Chem.* **1988**, *347*, 77. (c) Rosenthal, U.; Schulz, W. *Ibid.* **1987**, *321*, 103. (d) Capelle, B.; Dartiguenave, M.; Dartiguenave, Y.; Beauchamp, A. L. *J. Am. Chem. Soc.* **1983**, *105*, 4462. (e) Rees, W. M.; Churchill, M. R.; Fettinger, J. C.; Atwood, J. D. *J. Organomet. Chem.* **1987**, *7*, 1429.

(20) Stoutland, P. O.; Bergman, R. G.; Nolan, S. P.; Hoff, C. D. *Polyhedron* **1988**, *7*, 1429.

(21) Albright, T. A.; Burdett, J. K.; Whangho, M. H. *Orbital Interaction in Chemistry*; Wiley: New York, 1985.

Scheme III

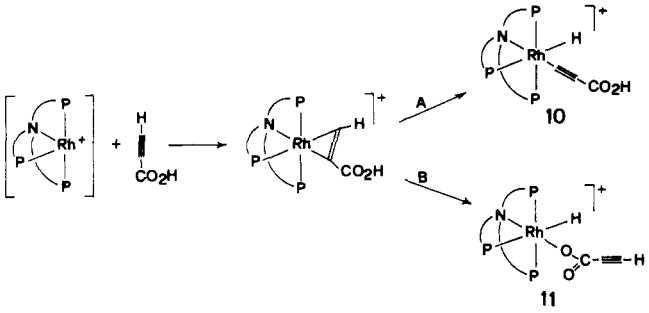

spectrum consists of an AM_2X splitting pattern with chemical shifts and coupling constants markedly different from those observed for the hydride acetylide complexes **4–9** [$\delta(P_A)$ = 16.89, $\delta(P_M)$ = 14.22 ppm; $J(PP)$ = 27.8, $J(P_ARh)$ = 150.4, $J(P_MRh)$ = 102.9 Hz] but somewhat in line with the NMR parameters found for the π-ethyl propiolate compound **20** at the same temperature. On standing, a slow reaction occurs as shown by the progressive appearance of the other two AM_2X patterns while the intensity of the starting AM_2X system diminishes. Parallelly, two multiplets in the hydride region (−7.59 and −7.09 ppm) appear in the ^1H NMR spectrum. The higher the temperature, the faster is the conversion of what is reasonable to consider the kinetic product, into the thermodynamic ones. Unfortunately, we were not able to isolate a pure sample of the kinetic product as the addition of *n*-pentane to a freshly prepared mixture of $[(NP_3)Rh]^+$ and $HC{\equiv}CCO_2H$ even at −40 °C resulted in the precipitation of a gummy mixture of three products. However, the IR spectrum of the mixture showed a band at 1800 cm^{-1} that can be assigned to a π-bonded acetylene group.[19] In contrast, addition of ethanol to a reaction mixture kept at room temperature for 30 min precipitates microcrystals of the two thermodynamic products, namely, $[(NP_3)Rh(H)(C{\equiv}CCO_2H)]BPh_4$ (**10**) and $[(NP_3)Rh(H)(O_2CC{\equiv}CH)]BPh_4$ (**11**), which were separated from each other by thick-layer chromatography. Evidently, the π-propiolic acid intermediate degrades via two almost equally favored pathways (**10** and **11** form in a 3:2 ratio as determined by NMR integration): pathway A, which leads to the expected hydrido acetylide species **10** via C–H bond activation and pathway B, which leads to the novel hydrido carboxylate species **11** via O–H oxidative addition (Scheme III).

Compounds **10** and **11** exhibit ^{31}P NMR AM_2X spin systems with quite different coupling constants and chemical shifts. In particular, the spectral features of **10** are in line with those found for all the other OCT Rh(III) acetylide complexes herein described (see Tables III and IV). The different fragmentation of propiolic acid at rhodium in **10** and **11** is clearly shown also by the IR spectra. As an example, $\nu(C{\equiv}C)$ in **10** is shifted to low energy by ca. 30 cm^{-1} as compared to the free alkyne, while it is practically unshifted in **11**. A complementary situation is observed for $\nu(C{=}O)$ of the carboxylic group (see Table I). In both compounds, the hydride ligand is located trans to the equatorial phosphorus of NP_3 rather than to nitrogen.

In conclusion, our experimental results show for the first time that also the activation of the substituent as it happens for the sp C–H bond requires preliminary π-coordination of the alkyne to the metal.

Reactivity of the Hydride Acetylide Complexes. Synthesis of σ-Acetylide Compounds. All of the hydride acetylide complexes are quite thermally stable and can be refluxed in THF or dioxane for hours with no apparent decomposition. Also, they exhibit a remarkable chemical stability as they remain intact even when treated in boiling THF either with strong donors like CO or MeCN or with molecules capable of oxidatively adding like H_2 and halocarbons.

Scheme IV

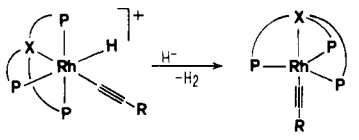

Scheme V

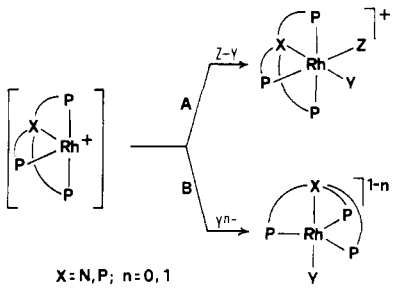

In contrast, most of the compounds react in THF with excess $NaBH_4$ dissolved in ethanol, yielding H_2 and the novel Rh(I) σ-acetylide complexes $[(L)Rh(C{\equiv}CR)]$ [L = NP_3, R = C_3H_7 (**22**), Ph (**23**), $SiMe_3$ (**24**), CH_2OH (**25**), CO_2Et (**26**); L = PP_3, R = C_3H_7 (**27**), Ph (**28**), $SiMe_3$ (**29**), CH_2OH (**30**), CHO (**31**), CO_2Et (**32**)] (Scheme IV).

We have found that increasing the electron-withdrawing character of the substituent shortens the reaction time necessary to completely convert the hydride alkynyl complexes into the corresponding σ-acetylides. As an example, the reduction of **9** to **26** (CO_2Et substituent) is completed in ca. 4 h, whereas the conversion of **15** into **29** ($SiMe_3$ substituent) requires ca. 12 h. A completely different behavior is exhibited by the two hydride ethynyl compounds **3** and **12**. By reaction with $NaBH_4$, they do not give the expected σ-ethynyl derivatives, instead the TBP hydrides **1** and **2** are formed in good yield, respectively, through the elimination of ethyne which was determined by GLC. Finally, the Rh(III) hydride acetylide complexes do not react with strong bases such as NEt_3 or Bu^tOK, thus demonstrating that the reactions with $NaBH_4$ are not simple deprotonations.

Compounds **22–32** are moderately air-stable in the solid state but decompose in solution unless air is excluded. They are soluble in common organic solvents in which they behave as nonelectrolytes. The presence of a terminal alkynyl ligand in all compounds is diagnostically evidenced by the infrared spectra which contain medium to strong absorbances due to the C≡C stretch in the region 2010–2100 cm^{-1}. The $^{31}P\{^1H\}$ NMR spectra exhibit canonical A_3X (NP_3 derivatives) or AM_3X (PP_3 derivatives) patterns, both of which are consistent with TBP geometries around rhodium (Table IV). Invariably, the acetylide ligand is located trans to the bridgehead atom of the tripodal ligands, in an axial position of the trigonal bipyramid. The presence in the intact form of the various functional groups on the alkynyl ligands (C_3H_7, $SiMe_3$, CH_2OH, CHO, CO_2Et) is shown by their typical ^1H NMR patterns (Table III). No signal in the hydride region is observed.

Discussion

$[Rh(\pi\text{-}HC{\equiv}CR)] \rightarrow [Rh(H)(C{\equiv}CR)]$ Rearrangement. The 16-electron fragments $[(NP_3)Rh]^+$ and

Scheme VI

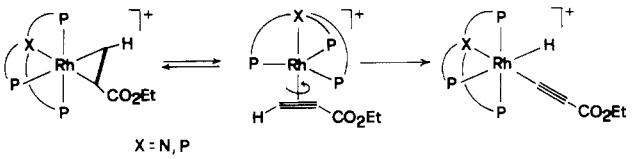

X = N, P

$[(PP_3)Rh]^+$ can be stabilized by two different types of reactions: (A) oxidative addition of various chemical bonds to give OCT complexes of rhodium(III); (B) ligand addition to give TBP complexes of rhodium(I) (Scheme V).[5,12]

1-Alkynes are expected to lie at the borderline between the two reagents as they can act either as oxidative addenda via C–H bond cleavage or as classical ligands which fill up the metal external shell up to 18 electrons. In the latter eventuality, a further distinction must be made since alkynes formally may oxidize the metals to give "metallacyclopropene" complexes. In this respect, it is not accidental that the metallacyclopropene structure is *favored by electron-withdrawing substituents on the alkyne and a tendency for the metal to be more stable in the higher oxidation state.*[19]

All of these considerations contribute to explain some of the results presented in this paper. When the alkyne substituent exhibits negligible electron-withdrawing character, hydride acetylide complexes of rhodium(III) are invariably obtained even at low temperature. In contrast, introducing a powerful electron-withdrawing group like $-CO_2Et$ or $-CO_2H$ makes the isolation of π-alkyne complexes feasible. The π-alkyne adducts are thermodynamically unstable in ambient temperature solutions in which they undergo irreversible insertion of rhodium across the sp C–H bond (or across the acidic O–H bond of propiolic acid). Interestingly, we have found that the $[Rh(\pi\text{-}HC{\equiv}CCO_2Et)] \rightarrow [Rh(H)(C{\equiv}CCO_2Et)]$ rearrangement is preceded at low temperature by a dynamic process involving $A_3X \rightleftarrows AM_2X$ (NP_3) and $AM_3X \rightleftarrows AM_2QX$ (PP_3) ^{31}P NMR spin systems. ^{31}P NMR AM_2X and AM_2QX patterns are typical of NP_3 and PP_3 complexes of rhodium with OCT structures whereas the A_3X and AM_3X splitting systems are readily assigned to TBP structures.[5] Conceptually, however, AM_2X and AM_2QX patterns may be originated also by TBP complexes in which the axial coligand is not symmetrical with respect to the equatorial phosphorus atoms. This may well be the case of **20** and **21** as the alkyne bears different terminal substituents. Accordingly, the evolution of the metal–substrate system $[(L)Rh]^+/HC{\equiv}CCO_2Et$ with the temperature increasing from −90 to +20 °C may be illustrated as shown in (Scheme VI) (L = NP_3, PP_3).

Whatever the low-temperature structure may be, the complexes appear TBP in ambient-temperature solutions. In this eventuality, provided a little energy, they are known to easily generate an occupied frontier σ-orbital upon slight displacement of a phosphorus donor in the equatorial plane of the trigonal bipyramid.[22] This hybrid, which substantially corresponds to the frontier σ-orbital of a d^8 ML_5 fragment, can be readily attacked by a variety of electrophiles, including acidic protons and C–H bonds from alkynes.[4,5,22] In conclusion, the Rh(I) TBP forms of **20** and **21** are excellent candidates for intramolecularly cleaving C–H as shown in Scheme VII (obviously, a similar mechanism can be proposed for the alternative O–H bond cleavage). According to this interpretation, it is now not

Scheme VII

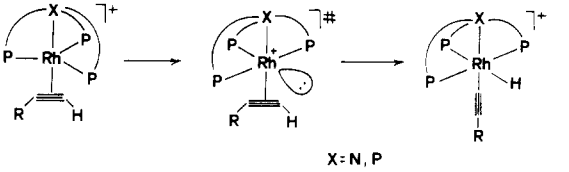

X = N, P

Scheme VIII

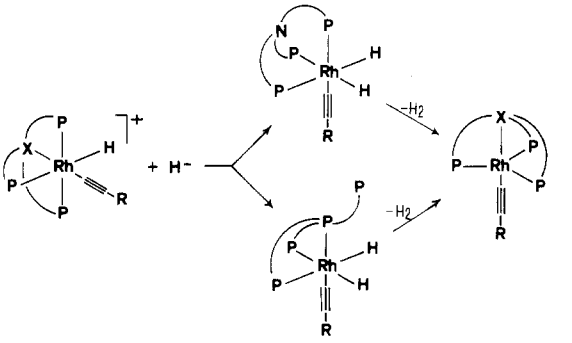

surprising that 1-alkynes bearing substituents less electron-withdrawing than CO_2Et or CO_2H and, therefore, less suitable than $HC{\equiv}CCO_2Et$ or $HC{\equiv}CCO_2H$ to stabilize π-alkyne species directly afford hydride acetylide complexes even at low temperature.

$[Rh(\pi\text{-}HC{\equiv}CR)] \rightarrow [Rh(H)(C{\equiv}CR)] \rightarrow [RhC{=}C(H)R]$ Rearrangement. In most instances, creation of a vacant coordination site at the metal on saturated complexes with NP_3 and PP_3 requires unfastening of one of the four donor atoms of the tripodal ligand.[5] Generally, NP_3 complexes attain coordinatively unsaturated structures by removing the nitrogen atom. In contrast, PP_3 complexes undergo preferential decoordination of a terminal phosphorus atom. However, metal complexes containing NP_3 or PP_3 acting as tridentate ligands most often have an exclusively transient nature. The pendant donor atom remains in close proximity of the metal and can easily displace a coligand or promote insertion reactions and reductive eliminations.[5] It is therefore reasonable to propose the mechanism shown in Scheme VIII to account for the formation of H_2 and the σ-acetylides **22–32** from the corresponding hydride acetylide species.

As a partial anticipation[23] of the chemistry of the present family of TBP σ-acetylides with NP_3, we report here that protonation by strong acids in THF invariably occurs at the β-carbon of the acetylide ligands to give stable TBP vinylidenes. These exhibit a rich chemistry: deprotonation by strong bases re-forms the starting acetylides; thermal decomposition gives H_2 and monocationic Rh(II) σ-acetylides; reaction with H^- yields Rh(I) σ-alkenyl derivatives.[24] In no case, however, did we observe formation of any of the Rh(III) cis hydride acetylide complexes herein presented. Similarly, we were not able to convert any of the hydride acetylides **3–9** into the corresponding vinylidene unless one considers a "conversion" the two-step reaction shown in III. Accordingly, as far as our systems

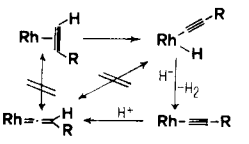

III

(22) (a) Bianchini, C.; Masi, D.; Mealli, C.; Meli, A.; Sabat, M.; Vizza, F. *Inorg. Chem.* **1988**, *27*, 3716. (b) Bianchini, C. *Comments Inorg. Chem.* **1988**, *8*, 27.

(23) Bianchini, C.; Laschi, F.; Ottaviani, F.; Peruzzini, M.; Zanello, P. *Organometallics* **1988**, *7*, 1660.

(24) To be submitted for publication.

are concerned, we conclude paraphrasing Silvestre and Hoffmann: *the hydrido-acetylide channel is a dead end, as far as eventual vinylidene production is concerned.*[2]

Acknowledgment. We are grateful to Dr. C. Mealli for the helpful discussion and to Mr. P. Innocenti and Mr. A. Traversi for technical assistance. Part of this work was supported by a grant from the CNR program "Progetto Finalizzato". We wish to thank also Conselleria de Cultura of Generalitat Valenciana for a grant that made J.A.R.'s stay in Firenze possible.

Supplementary Material Available: Positional and thermal parameters for anisotropically refined atoms (Table S1), positional and thermal parameters for isotropically refined atoms (Table S2), and final positional parameters for hydrogen atoms for **3**·1.5 THF (Table S3) (5 pages); a listing of observed and calculated structure factors for **3**·1.5 THF (22 pages). Ordering information is given on any current masthead page.

Synthesis and Properties of (*O*-Acyl imidato)carbene Complexes of Chromium, Molybdenum, and Tungsten

Louis S. Hegedus,* Lisa M. Schultze, and John Montgomery

Department of Chemistry, Colorado State University, Fort Collins, Colorado 80523

Received January 27, 1989

A number of (*O*-acyl imidato)carbene complexes of chromium, molybdenum, and tungsten were prepared by the acylation of aminocarbenes or by the reaction of acetoxycarbenes with amides. These relatively unstable complexes had unusual spectroscopic properties and underwent thermal reactions with imines to give low yields of 3-azetidinones. Two amido chromium carbene complexes were also prepared. These were quite unstable, resembling acetoxycarbenes, and readily decomposed. An (*N*-carbobenzoxyamino)carbene was also prepared. It was the most stable of these carbenes and underwent reactions typical of aminocarbene complexes.

Recently a novel photochemical reaction between imines and "Fischer" carbene complexes of chromium to produce β-lactams was developed in these laboratories (eq 1).[1] A

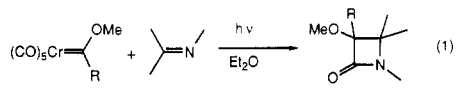

(1)

wide range of imines, including thiazines, benzothiazines, and thiazolines, as well as quinoline and dihydroisoquinolines underwent this reaction, producing β-lactams in excellent yield. Under similar conditions, azirines produced *N*-vinylimidates,[2] azobenzenes produced 1,2- and 1,3-diazetidinones,[3] and, with molybdenum carbene complexes, oxazoles and oxazolines produced β-lactams.[4] These studies utilized methoxymethyl- and methoxyphenylcarbene complexes since these were most readily accessible by classic Fischer methodology,[5] the reaction of an organolithium reagent with chromium hexacarbonyl, followed by treatment of the thus formed "ate" complex with trimethyloxonium tetrafluoroborate.[6] This resulted in the formation of β-lactams having methoxy and alkyl substituents α to the carbonyl group. However, most biologically active β-lactams have amide functionality at this position,[7] requiring the use of (*N*-acylamino)carbene complexes in the above synthesis.

Aminocarbene complexes are readily prepared by the reaction of alkoxycarbene complexes with amines,[8] a simple exchange process analogous to the conversion of organic esters to amides. However, amides do *not* undergo this exchange process with alkoxycarbene complexes, and amidocarbene complexes are not available by this route.[9] Acetoxycarbene complexes, prepared by O-acylation of acyl "ate" complexes, are similar to mixed anhydrides and are considerably more reactive toward weak nucleophiles than are the corresponding alkoxycarbenes.[10,11] The use of amides as nucleophiles would lead to the desired amidocarbene complexes, if successful (see below).

Because of extensive delocalization of the nitrogen lone pair of electrons into the electron-deficient chromium system,[12] direct acylation of aminocarbene complexes was not feasible. However, aminocarbene complexes have been *alkylated* by deprotonation at nitrogen with a strong base (e.g., CH_3Li, LDA) followed by N-alkylation with active alkylating agents (e.g., CH_3I, Me_3OBF_4).[13,14] The use of acyl halides or anhydrides as electrophiles would again result in formation of the desired amidocarbene complexes

(1) Hegedus, L. S.; McGuire, M. A.; Schultze, L. M.; Yijun, C.; Anderson, O. P. *J. Am. Chem. Soc.* **1984**, *106*, 2680.
(2) Hegedus, L. S.; Kramer, A.; Yijun, C. *Organometallics* **1985**, *4*, 1747.
(3) Hegedus, L. S.; Kramer, A. *Organometallics* **1984**, *3*, 1263.
(4) Hegedus, L. S.; Schultze, L. M.; Toro, J.; Yijun, C. *Tetrahedron* **1985**, *41*, 5833.
(5) Aumann, R.; Fischer, E. O. *Chem. Ber.* **1960**, *101*, 954.
(6) We have recently developed efficient syntheses of $(CO)_5Cr{=}C(NR_2)H$ complexes. See: Borel, C.; Hegedus, L. S.; Krebs, J.; Satoh, Y. *J. Am. Chem. Soc.* **1987**, *109*, 1101. Imwinkelried, R.; Hegedus, L. S. *Organometallics* **1988**, *7*, 702.
(7) Durkheimer, W.; Blumbach, J.; Lattrell, R.; Scheunemann, K. H. *J. Angew. Chem., Int. Ed. Engl.* **1985**, *24*, 180.
(8) (a) Heckl, B.; Werner, H.; Fischer, E. O. *Angew. Chem., Int. Ed. Engl.* **1968**, *7*, 817. (b) Werner, H.; Fischer, E. O.; Heckl, B.; Kreiter, C. G. *J. Organomet. Chem.* **1971**, *28*, 367.
(9) Connor, J. A.; Fischer, E. O. *J. Chem. Soc. A* **1969**, 578.
(10) Connor, J. A.; Jones, E. M. *J. Chem. Soc. A* **1971**, 3368.
(11) Semmelhack, M. F.; Bozell, J. J.; Sato, T.; Wulff, W.; Spiess, E.; Zask, A. *J. Am. Chem. Soc.* **1982**, *104*, 5850.
(12) Connor, J. A.; Mills, O. S. *J. Chem. Soc. A* **1969**, 334.
(13) Moser, E.; Fischer, E. O. *J. Organomet. Chem.* **1968**, *15*, 147.
(14) Casey, C. P.; Vollendorf, N. W.; Haller, K. J. *J. Am. Chem. Soc.* **1984**, *106*, 3755.

0276-7333/89/2308-2189$01.50/0